

This paper was published as part of the

Materials for Detection web theme issue



With *Analyst* and *Journal of Materials Chemistry*

Immobilisation of proteins at silicon surfaces using undecenylaldehyde: demonstration of the retention of protein functionality and detection strategies

Qi Hong, Celia Rogero, Jeremy H. Lakey, Bernard A. Connolly, Andrew Houlton and Benjamin R. Horrocks
[DOI: 10.1039/B813328J/Analyst](https://doi.org/10.1039/B813328J/Analyst)

SERRS coded nanoparticles for biomolecular labelling with wavelength-tunable discrimination

Fiona McKenzie, Andrew Ingram, Robert Stokes and Duncan Graham
[DOI: 10.1039/B813821D/Analyst](https://doi.org/10.1039/B813821D/Analyst)

Functional DNA directed assembly of nanomaterials for biosensing

Zidong Wang and Yi Lu
[DOI: 10.1039/b813939c/Journal of Materials Chemistry](https://doi.org/10.1039/b813939c/Journal_of_Materials_Chemistry)

Detection of drugs and their metabolites in dusted latent fingerprints by mass spectrometry

Frederick Rowell, Katherine Hudson and John Seviour
[DOI: 10.1039/B813957C/Analyst](https://doi.org/10.1039/B813957C/Analyst)

Highly encoded one-dimensional nanostructures for rapid sensing

Sung-Kyoung Kim and Sang Bok Lee
[DOI: 10.1039/b814408g/Journal of Materials Chemistry](https://doi.org/10.1039/b814408g/Journal_of_Materials_Chemistry)

Nanomaterials for ultrasensitive electrochemical nucleic acids biosensing

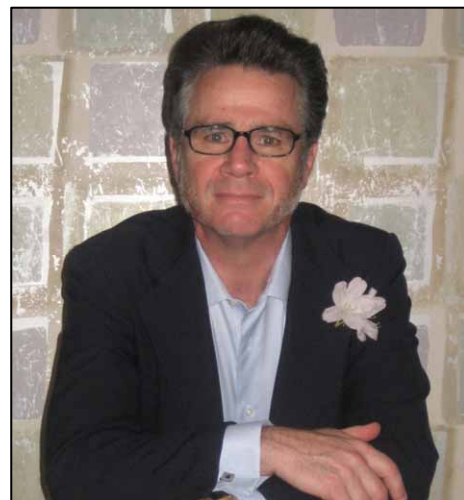
Heather Lord and Shana O. Kelley
[DOI: 10.1039/b814569e/Journal of Materials Chemistry](https://doi.org/10.1039/b814569e/Journal_of_Materials_Chemistry)

Functional nanomaterial-based amplified bio-detection strategies

Jongho Jeon, Dong-Kwon Lim and Jwa-Min Nam
[DOI: 10.1039/B816690K/Journal of Materials Chemistry](https://doi.org/10.1039/B816690K/Journal_of_Materials_Chemistry)

Development of a piezoelectric sensor for the detection of methamphetamine

Maria Romero Guerra, Iva Chianella, Elena V. Piletska, Kal Karim, Anthony P. F. Turner and Sergey A. Piletsky
[DOI: 10.1039/B819351G/Analyst](https://doi.org/10.1039/B819351G/Analyst)



Guest Editor:
Professor Charles Martin,
University of Florida

You can read the rest of the articles in this issue at

www.rsc.org/publishing/detection

Polymerization of a boronate-functionalized fluorophore by double transesterification: applications to fluorescence detection of hydrogen peroxide vapor†

Jason C. Sanchez and William C. Trogler*

Received 9th June 2008, Accepted 20th August 2008

First published as an Advance Article on the web 29th September 2008

DOI: 10.1039/b809674k

The double transesterification polymerization of 3',6'-bis(pinacolatoboron)fluoran and pentaerythritol is reported. A model dimeric compound was synthesized to demonstrate the effectiveness of bis-diols to undergo a double transesterification, which is driven by formation of the energetically favored six-membered di-ester ring from a monomer containing a five-membered di-ester ring. This synthetic procedure provides a new route to boronate based polymers, avoiding unstable boronic acid monomers. Formation of poly-3',6'-bis(1,3,2-dioxaborinane)fluoran, with a molecular weight of 10 000, is complete after 48 h at 50 °C. The thermodynamic stability of the six-membered boronic ester rings present in the polymer backbone also improves the stability of the polymer and its resistance to oxidation under ambient and UV light conditions. A surface detection method for the analysis of H₂O₂ vapor by a fluorescence turn-on response was explored. The fluorescent response results from oxidative deprotection of the boronate functionalities forming green luminescent fluorescein. Detection limits as low as 3 ppb were observed for H₂O₂ over an 8 h period. Detection of H₂O₂ in liquids can also be carried out through spot tests at concentrations as low as 1 ppm after 5 min. This new vapor-phase sensor for H₂O₂ provides a robust, low-cost alternative to current technology for potential applications as a self-integrating sensor for the detection of H₂O₂ as well as the direct monitoring of H₂O₂ levels in areas such as cargo shipments, chemical facilities, and pulp bleaching.

Introduction

Detection and analysis of explosive materials and formulations has become an integral part of national and global security.¹ The lack of robust, low-power, portable detection devices for the rapid on-site screening of both common and suspicious chemicals, materials, cargo, and persons, has driven the need for improved sensor devices, such as photoluminescent sensors.² However, improvised peroxide explosives are not detectable by these technologies.³ The two most common such materials are triacetone triperoxide (TATP) and hexamethylene triperoxide diamine (HMTD) (Fig. 1). These chemicals do not contain nitro or aromatic functionalities but incorporate cyclic peroxides that are stable enough to be transported, but are moderately shock sensitive (Table 1).⁴ Both TATP and HMTD can be synthesized easily with common chemicals, so starting materials do not need to be harvested from munition stockpiles or stolen from chemical factories or institutions.⁵ Current detection methods for TATP and HMTD include separation techniques, ion detection, and UV-vis and fluorescence response to photochemical decomposition.⁶ These methods either involve complex spectroscopic evaluation, multiple steps for detection, or a complex matrix of

organic and aqueous solvents. Sensor efforts have focused on targeting hydrogen peroxide (H₂O₂) produced through UV⁷ or acid-catalyzed⁸ decomposition of TATP or HMTD. Bulk TATP and HMTD may also include residual H₂O₂ left over from their synthesis.

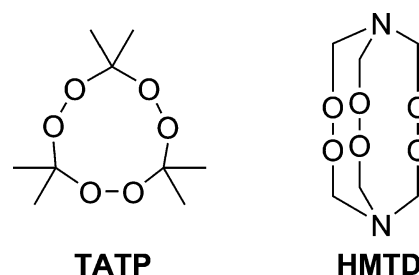


Fig. 1 Chemical structures of triacetone triperoxide (TATP) and hexamethylene triperoxide diamine (HMTD).

Table 1 Properties of organic peroxide based explosives compared with TNT

Explosive	Type	Melting Point/°C	P_{vap} /Torr	Detonation velocity/m s ⁻¹
TATP	Primary	98	5.3×10^{-2}	5300
HMTD	Primary	148	NA	5100
TNT ^a	Secondary	81	5.8×10^{-6}	6850

^a Nitroaromatic based explosive for comparison.

Department of Chemistry and Biochemistry, University of California at San Diego, 9500 Gilman Drive, La Jolla, California 92093-0358, USA. E-mail: wtrogler@ucsd.edu

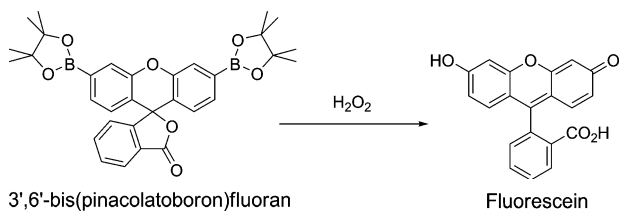
† Electronic supplementary information (ESI) available: The fluorescence spectra of PolyF-1 (10 μg cm⁻² on filter paper) after exposure to UV light and ambient conditions, and the ¹H NMR and ¹³C NMR for dimer **1**. See DOI: 10.1039/b809674k

While current H_2O_2 detection methods have advanced in sensor sensitivity, they typically involve liquid sampling media and evaluation.⁹ To overcome these limitations, we have been interested in sensors that target vapor-phase H_2O_2 .

Use of H_2O_2 in paper pulp bleaching, speciality chemical synthesis, and chemical disinfection also require monitoring of vapor H_2O_2 levels¹⁰ due to the acute toxicity inherent in even small doses of H_2O_2 (1 ppm).¹¹ Current methods for the detection of H_2O_2 vapor rely on chemiresistive,¹² electrochemical,¹³ colorimetric,¹⁴ and vibrational spectroscopy analysis.¹⁵

Fluorimetric sensing is a potentially promising approach. Current methods that focus on the use of fluorescence to monitor the presence of H_2O_2 include water-soluble FRET-based polyelectrolytes,¹⁶ deprotection of fluorescein derivatives,¹⁷ and benzofurans.¹⁸ These methods involve solution-phase determination of H_2O_2 for biological assays. One application that provides very high selectivity for H_2O_2 detection is the oxidative deprotection of boronic ester substituted fluoran, xanthanone, and phenoxazine derivatives, which have been synthesized by Chang and co-workers.¹⁹ These functional fluorophores are highly specific for the detection of H_2O_2 in biological systems. The sensors are utilized in a buffered aqueous media, showing good stability toward common interferents. The boronic ester functionalized fluoran shows the greatest fluorescence response due to the high quantum efficiency of fluorescein produced by the H_2O_2 specific oxidation of the two boronic ester functionalities (Scheme 1). The simplicity, sensitivity, and selectivity of this system make it an ideal candidate for vapor-phase detection of H_2O_2 . However, the thin-film stability and processability of the 3',6'-bis(pinacolatoboron)fluoran monomer limits its use in solid-state sensor technology.

We report here the synthesis of poly-3',6'-bis(1,3,2-dioxaborinane)fluoran (**PolyF-1**) by double transesterification polymerization of 3',6'-bis(pinacolatoboron)fluoran and pentaerythritol. This is the first synthesis, to the best of our knowledge, which uses a double transesterification of boronic esters as a polymerization technique. Similar polymerization routes have used the condensation polymerization of boronic acids with bis-diols. This technique has been employed in the synthesis of oligomers,²⁰ polymers,²¹ and macrocycles²² for use as self-repairing materials and in thermal dehydration crosslinking applications. The drawback is that boronic acids are unstable under ambient conditions and require azeotropic or Dean–Stark removal of water for the reaction to proceed. The instability and complex synthetic issues may be avoided through the use of transesterification. In addition, direct conversion of a five-membered cyclic boronic ester to a six-membered cyclic boronic ester yields a highly stable polymer structure.²³ **PolyF-1** was screened for its



Scheme 1 Selective oxidation of 3',6'-bis(pinacolatoboron)fluoran by H_2O_2 forming the fluorescein fluorophore.

ability to detect vapor-phase H_2O_2 by fluorimetric analysis and it shows promise as a sensitive and selective polymeric sensor film for the detection of trace quantities of H_2O_2 in both liquid and vapor phases.

Experimental

General information

All synthetic manipulations were carried out under an atmosphere of dry argon gas using standard Schlenk techniques unless otherwise noted. Dry solvents were purchased from Aldrich Chemical Co. Inc. and used after purification with an MBraun Auto Solvent Purification System. Pentaerythritol (98%) was purchased from Acros Organics and used as received. For dosing studies, 30 wt% H_2O_2 in water (Acros) was purchased, using a fresh solution for every dosing run. Hydrogen peroxide solutions were assayed *via* iodometric titration and the average peroxide weight percentage was $27.1 \pm 2.0\%$. Di-*t*-butyl peroxide (Aldrich, 98%) and benzoyl peroxide (Aldrich, 97%) were used as purchased and stored at 2–6 °C under inert gas. The following were prepared by literature methods: 4,4,5,5-tetramethyl-2-*p*-tolyl-1,3,2-dioxaborolane²⁵ and 3',6'-bis(pinacolatoboron)fluoran.¹⁹ NMR data were collected using a Varian Mercury Plus spectrometer and 9.4 T superconducting magnet (399.911 MHz for ^1H and 100.52 MHz for ^{13}C NMR). A Perkin–Elmer LS 45 luminescence spectrometer was used to record fluorescence emission and excitation spectra. GPC data was obtained with the use of a Viscotek GPCmax VE 2001 GPC; molecular weights were recorded relative to polystyrene standards and low molecular weight silole monomers and dimers. The data were fitted using Origin8.

Periodic acid test for *cis*-diols

The periodic acid test can be used to monitor the presence of 1,2-diols. The transesterification between pinacolatoboron and pentaerythritol produces pinacol as the reaction proceeds. This 1,2-diol can be detected selectively over pentaerythritol through its oxidative cleavage yielding ketone and iodate products. The presence of iodate can then be determined by formation of a white precipitate of AgIO_3 in the presence of Ag^+ . To a periodic acid reagent (2 mL, 0.1 M) was added 1 drop of nitric acid (0.1 M) and 1 drop of solution taken from the reaction mixture. This was stirred for 10 s and 2 drops of AgNO_3 was added. The solution was stirred for 5 s and the resulting white precipitate confirms the presence of pinacol.

Peroxide detection

Thin films of **PolyF-1** were prepared by drop-casting the polymer from a CHCl_3 solution onto thin sheets of Whatman2 filter paper (4 cm^2). The filter paper provides a porous sampling substrate that maximizes the surface area of the polymer exposed to the H_2O_2 analyte. Concentrations of 2.5, 10, and 40 $\mu\text{g cm}^{-2}$ were evaluated for **PolyF-1**. The films are not visible to the naked eye and show no luminescence over a 5 h period after exposure to UV light and ambient air. Detection of H_2O_2 was initially carried out in the vapor phase using a modified inert gas flow system. Argon was bubbled through a dilute solution of H_2O_2 in water, and the

vapor concentration was calculated based on temperature and mole fraction of H₂O₂ in the solution.²⁴ The inert gas flow was directed into a sealed chamber through a Teflon tube. Cotton was placed inside the chamber to provide a more consistent saturation of H₂O₂. The chamber was purged for 10 min before each film exposure to ensure that an equilibrium vapor concentration was reached. The films were placed into the sealed chamber and fluorescence spectra were recorded upon removal of the film at various time intervals. The film was placed into a solid-support scaffold on the fluorimeter to ensure repeatability of the site of photo-excitation on the film. H₂O₂ vapor concentrations of 91, 29, 3.8, 2.9, and 1.2 ppm were evaluated for both **PolyF-1** and the fluoran monomer at a film concentration of 10 μg cm⁻². Solutions of H₂O₂ were also examined at concentrations of 7 ppt, 1 ppt, 300 ppm, and 30 ppm to show application of **PolyF-1** as both a vapor-phase sensor for H₂O₂ and a qualitative screening test for the presence of H₂O₂ in suspicious solutions.

3,9-Di-*p*-tolyl-2,4,8,10-tetraoxa-3,9-diborospiro[5.5]undecane (**1**)

To a stirring methanol solution of 4,4,5,5-tetramethyl-2-*p*-tolyl-1,3,2-dioxaborolane (4 mL, 115 mM) was added an aqueous solution of pentaerythritol (1 mL, 0.23 mM). The mixture was stirred at room temperature for 12 h. Reaction progress was monitored by both TLC and a periodic acid test. After 8 h the solution became cloudy and a white precipitate formed. The solid was extracted with methylene chloride, washed with brine and water, and evaporated to dryness yielding a white powder (50 mg, 65%). ¹H NMR (CDCl₃, ppm): δ 7.69 (d, 4H, Ph-*H*), 7.18 (d, 4H, Ph-*H*), 4.05 (s, 8H, CH₂), 2.37 (s, 6H, CH₃); ¹³C{¹H} NMR (CDCl₃, ppm): δ 141.4, 134.1, 128.6, 65.0, 36.8, 21.9; mp = 259–261 °C; Calcd for C₁₉H₂₂O₄B₂: C 67.9, H 6.60; Found: C 68.2, H 6.84.

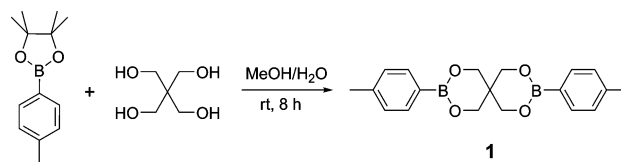
Poly-3',6'-bis(1,3,2-dioxaborinane)fluoran (**PolyF-1**)

To a stirring methanol solution of 3',6'-bis(pinacolatoboron)fluoran (4 mL, 45 mM) under ambient conditions was added an aqueous solution of pentaerythritol (1 mL, 0.18 mM). The mixture was stirred at 50 °C for 48 h. Reaction progress was monitored by TLC and a periodic acid test. The colorless solution was extracted with methylene chloride, washed with brine and water, and the organic extract was evaporated to dryness. The resulting off-white solid was washed with cold methanol, yielding a white powder (61 mg, 75%). ¹H NMR (400.053 MHz, CDCl₃): δ 8.03 (m, 1H, Ph-*H*), 7.73 (br d, 2H, Ph-*H*), 7.60 (m, 2H, Ph-*H*), 7.43 (m, 2H, Ph-*H*), 7.06 (m, 1H, Ph-*H*), 6.85 (br d, 2H, Ph-*H*), 4.07 (br s, 8H, CH₂); ¹³C{¹H} NMR (100.59 MHz, CDCl₃): δ 163.4, 135.4, 130.0, 129.6, 127.1, 125.4, 123.9, 84.5, 65.1, 45.9, 30.1; Calcd for C₂₅H₁₈O₇B₂: C 66.4, H 4.01; Found: C 66.5, H 4.4.

Results and discussion

Synthesis and characterization

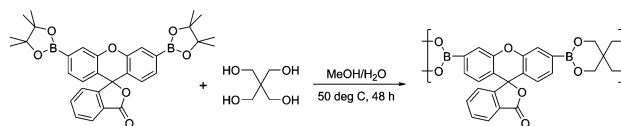
Transesterification of heterocyclic boronic esters is traditionally applied for the functionalization or protection of complex organic frameworks. There is much known about this process



Scheme 2 Synthesis of model dimer **1** by double transesterification to form six-membered rings.

and a recent review by Roy and Brown highlights structural effects of both the boronate and diol on the reaction progress.²³ One conclusion drawn from this study was the increased thermodynamic stability observed for six-membered ring boronic esters over five-membered ring boronic esters. This concept has been used for monomer functionalization but has yet to be applied as a route to stabilized boronate polymers. To demonstrate the viability of boronate double transesterification as a polymerization technique, a model dimer complex (**1**) was synthesized according to Scheme 2. 4-(Pinacolatoboron)toluene was used to mimic common arylboronates that may be used as comonomers for polymerization and pentaerythritol was used as the bis-diol to demonstrate the viability of a double transesterification of two five-membered ring boronic esters. The reaction proceeded smoothly at room temperature in MeOH–H₂O over 8 h. The presence of H₂O is important for the solubility of pentaerythritol and its presence as a co-solvent does not hinder the reaction progress as it does during condensation polymerization of boronic acids. The percentage of water was adjusted to ensure solubility of both reactants. Reaction progress was monitored by both TLC and a periodic acid test for the presence of *cis*-diols (see Experimental). The reaction was complete after 8 h with a 65% yield. Dimer **1** was characterized by ¹H NMR and ¹³C NMR analysis. The ¹H NMR shows a singlet (δ 4.05 ppm) representing the methylene groups of the pentaerythritol fragment. This singlet integrates with the methyl resonance of the toluene endgroups (δ 2.37 ppm) at a ratio of 4 : 3, respectively. There is no detectable pinacol, confirming the effectiveness of the purification process. Dimer **1** shows superior thermal stability (mp = 259–261) and shelf life compared to the 4-(pinacolatoboron)toluene while maintaining its solubility in many common organic solvents.

The promising results seen by the preceding synthesis of dimer **1** led us to consider this technique for polymerization of 3',6'-bis(pinacolatoboron)fluoran. The double transesterification polymerization of 3',6'-bis(pinacolatoboron)fluoran and pentaerythritol was carried out in MeOH–H₂O at 50 °C for 48 h (Scheme 3). Again, a periodic acid test was used to monitor the formation of pinacol. The polymer (**PolyF-1**) was extracted with methylene chloride and washed with H₂O. The organic solvent was removed under vacuum and the resulting light yellow powder



Scheme 3 Synthesis of **PolyF-1** by double transesterification to form six-membered boronic ester rings.

was purified by cold MeOH washings to produce a white solid in good yield (75%). Several washings are required to fully remove the excess pinacol. This was the optimum result obtained after varying the reaction temperature, water content, and diol-monomer ratio. The molecular weight of **PolyF-1** was determined to be 10 000 by GPC with a polydispersity index (PDI) of 1.5. This polymer is thermally stable and non-luminescent. The ^1H NMR spectrum shows the presence of the pentaerythritol and the absence of the pinacol protecting group. Both ^1H and ^{13}C NMR show the presence of the fluoran comonomer in the polymer.

Detection of hydrogen peroxide

Detection of vapor-phase H_2O_2 was evaluated using thin-films of **PolyF-1** drop-cast onto a Whatman2 porous sampling substrate to increase the surface area for polymer-analyte interactions. Polymer films were maintained at $10\ \mu\text{g cm}^{-2}$ throughout the study. Both $2.5\ \mu\text{g cm}^{-2}$ and $40\ \mu\text{g cm}^{-2}$ films of **PolyF-1** were tested for their sensor effectiveness; however, the $10\ \mu\text{g cm}^{-2}$ film shows the best results when considering sensor stability and response while limiting the quantity of polymer used. A modified flow system using an inert carrier gas was used to achieve constant equilibrium vapor concentrations of H_2O_2 (see Experimental). Vapor concentrations of H_2O_2 were calculated using published data.²⁴ Time-dependent fluorescence spectra were taken on exposure of the **PolyF-1** film to H_2O_2 at concentrations of 91, 29, 3.8, 2.9, and 1.2 ppm. A representative fluorescence response plot for exposure of **PolyF-1** to 2.9 ppm H_2O_2 is seen in Fig. 2. An 8-fold increase in fluorescence intensity (510 nm) is observed over a 3.5 h period for 2.9 ppm H_2O_2 . The fluorescence spectrum observed is nearly identical to the fluorescence emission of a thin film of fluorescein deposited on the porous substrate. The decomposition of the **PolyF-1** upon exposure to H_2O_2 was monitored by GPC, showing the presence of oligomers ($M_w = 700$, PDI = 1.8) after 30 min of H_2O_2 exposure. The sensor reaction proceeds by an oxidative deprotection of the boronic ester functionalities, forming fluorescein from fluoran (Scheme 1).

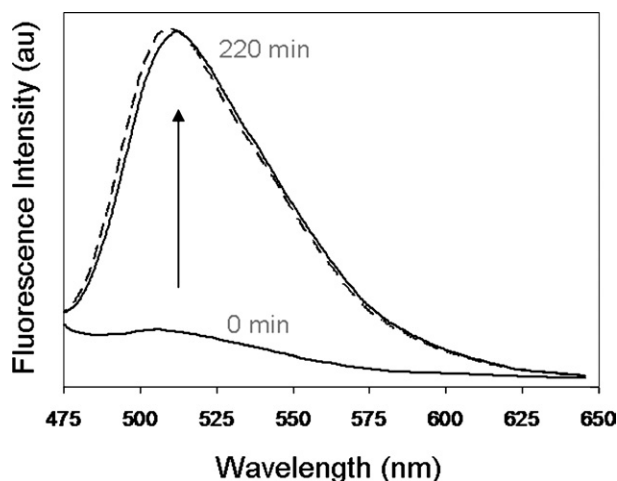


Fig. 2 Fluorescence response of a $10\ \mu\text{g cm}^{-2}$ film of **PolyF-1** to 2.9 ppm of H_2O_2 vapor after 220 min. Solid line at 0 min represents the baseline fluorescence intensity of the **PolyF-1** film. The dashed line represents the fluorescence emission of $100\ \mu\text{g cm}^{-2}$ of fluorescein.

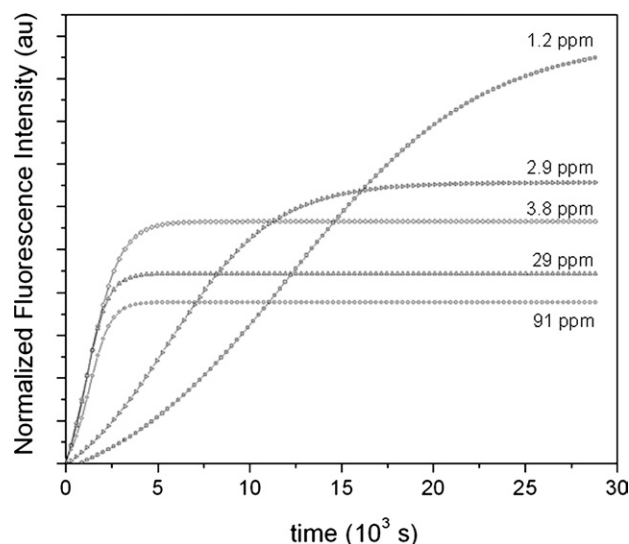


Fig. 3 Fluorescence trace of $10\ \mu\text{g cm}^{-2}$ **PolyF-1** exposed to various vapor concentrations of H_2O_2 .

The data obtained at varying concentrations of H_2O_2 is summarized in Fig. 3. At high vapor concentrations of H_2O_2 (>3.8 ppm) there is a rapid initial fluorescence response of the **PolyF-1** film on exposure to H_2O_2 . After ~ 1 h, a maximum fluorescence intensity is reached for each H_2O_2 concentration. At low H_2O_2 vapor concentrations (<2.9 ppm), there is a slow initial fluorescence response followed by a gradual increase in the time required to reach a maximum fluorescence intensity. However, the threshold for the maximum change in fluorescence intensity increases as the concentration of H_2O_2 decreases (Table 2). This inverse response is unique to this system. Typical turn-on fluorescence response scales proportionally with the concentration of analyte. In this case, there is an inverse relationship between the maximum fluorescence response and H_2O_2 concentration, which may be explained by the bleaching effect that H_2O_2 has on organic materials, especially at high concentrations. At high vapor concentrations, pseudo first order kinetics in H_2O_2 are expected (Fig. 4). However, there is also apparent competitive decomposition of the organic fluorophore with the excess H_2O_2 . This competing degradation prevents the maximum fluorescence response from being reached at high concentrations of H_2O_2 . While the kinetics at high concentrations of H_2O_2 are pseudo first

Table 2 Summary of **PolyF-1** ($10\ \mu\text{g cm}^{-2}$) fluorescence responses on exposure to H_2O_2 vapor

$[\text{H}_2\text{O}_2]/\text{ppm}$	$k^a/10^{-4}\ \text{s}^{-1}$	Flu. intensity at ∞ (I_∞) ^b	Time to reach $I_\infty/10^3\ \text{s}^c$
91	12	18.9	3.0
29	12	22.2	3.6
3.8	10	28.3	4.2
2.9	7.0	32.4	13
1.2	3.0	49.6	24

^a Derived from first order kinetic plots seen in Fig. 4. ^b Calculated from the exponential growth fit (eqn 2) of the time-dependent fluorescence trace of **PolyF-1** exposed to various concentrations of H_2O_2 (Fig. 3). ^c Time to reach within 3σ of I_∞ .

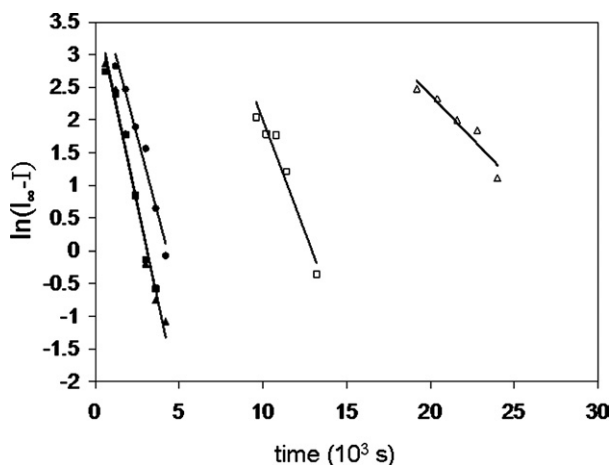


Fig. 4 First order kinetics plot of the fluorescence response of **PolyF-1** exposed to 91 ppm H_2O_2 (■, $R^2 = 0.98$), 29 ppm H_2O_2 (▲, $R^2 = 0.98$), 3.8 ppm H_2O_2 (●, $R^2 = 0.97$), 2.9 ppm H_2O_2 (□, $R^2 = 0.94$), and 1.2 ppm H_2O_2 (△, $R^2 = 0.94$). The apparent rate constant (k) is derived from the slope of the linear regression fit. At low concentrations of H_2O_2 , the reaction deviates from first order kinetics in H_2O_2 .

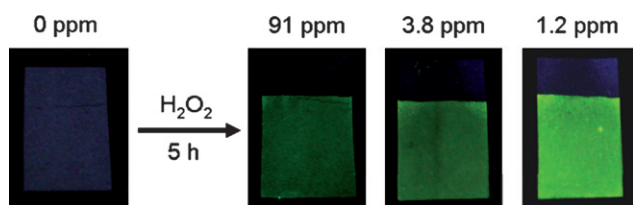


Fig. 5 Images of the fluorescence response of $10 \mu\text{g cm}^{-2}$ **PolyF-1** to various concentrations of H_2O_2 vapor over a 5 h period. An increase in fluorescence intensity is observed at lower concentrations of H_2O_2 providing a highly sensitive sensor response.

order, a change in kinetics is observed at around 2.9 ppm H_2O_2 . At lower concentrations the reaction begins to slow based on the decrease in the molar ratio of H_2O_2 to **PolyF-1**. At the same time, H_2O_2 is more readily consumed in the more energetically favored oxidative deprotection reaction and oxidative decomposition of the organic fluorophore begins to decrease. This causes a continual increase in the maximum fluorescence intensity (I_∞) at decreasing concentrations of H_2O_2 (Fig. 5). The reaction is also time-dependent, showing much longer exposure times to reach I_∞ at lower concentrations of H_2O_2 , so there is no problem distinguishing between high and low concentrations of H_2O_2 .

The films of **PolyF-1** were also screened for their stability under ambient UV light. This is relevant for real world interferences and film stability over time. **PolyF-1** shows a minimal fluorescence response under ambient conditions (0.06%) or UV light exposure (0.5%) over a period of 5 h. This demonstrates the good photo-stability of the films, as well as their stability to atmospheric oxidizers that may be created in the presence of UV light. The data collected for the UV light control experiment was used to calculate the standard deviation ($\sigma = 0.24$) for the film stability at 0 ppm H_2O_2 (Fig. S1, ESI†). This standard deviation was used to calculate the time at which a detectable signal is achieved for a given concentration of H_2O_2 .

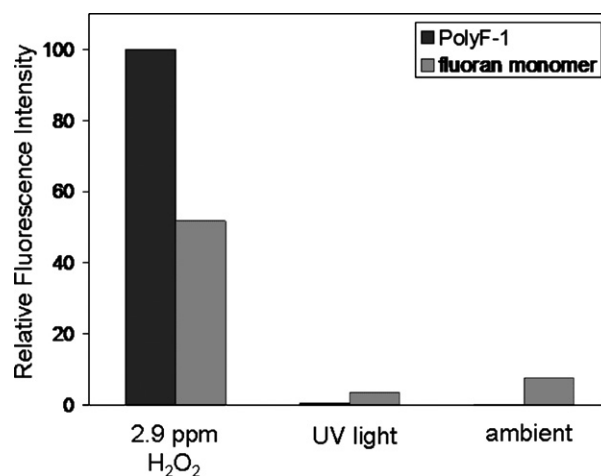


Fig. 6 Fluorescence responses of a $10 \mu\text{g cm}^{-2}$ film of **PolyF-1** and the same mass of 3',6'-bis(pinacolatoboron)fluoran (fluoran monomer) to 2.9 ppm H_2O_2 , UV light, and ambient conditions over a 5 h period. **PolyF-1** shows a greater fluorescence response to H_2O_2 and is more stable as a thin film than the fluoran monomer.

The monomer material 3',6'-bis(pinacolatoboron)fluoran was also screened for its ability to detect H_2O_2 . This experiment was performed to determine whether there is an advantage to using the polymeric version of the sensor as **PolyF-1**. The fluoran monomer shows decreased stability when exposed to both ambient conditions (7.4% of the maximum fluorescence intensity) and UV light (3.4%), as compared with **PolyF-1**. The response to H_2O_2 is also weaker, accounting for only a 4-fold increase in fluorescence intensity on exposure to 2.9 ppm H_2O_2 as compared to an 8-fold increase for **PolyF-1** (Fig. 6). The stability of the six-membered boronic ester functionalities in **PolyF-1** may assist in directing the peroxide oxidation to deprotection of the boronic ester rather than decomposing the organic framework. In addition, processability of the monomer material for thin-film application is much more difficult than for **PolyF-1**.

Quantifying the detection results of a vapor phase turn-on fluorescence sensor based on the chemical modification of a polymer thin film presents a unique challenge. The sensor response is proportional to time but inversely proportional to H_2O_2 concentration. The increase in signal response with decreasing concentrations of H_2O_2 prevents typical analysis of the detection response. In order to better quantify this system, the fluorescence intensity at infinity (I_∞), calculated from a single exponential growth (eqn 1), was fitted to the time-dependent fluorescence response data (Fig. 3). Using I_∞ , a correlation between the time required to reach within 3σ of I_∞ and H_2O_2 concentration can be made (Fig. 7). The data was fit to an exponential decay with an R^2 of 0.999 (eqn 2). From this fit a detection limit of 0.7 ppm (at time = ∞) can be determined. This limit is based on the maximum fluorescence response from **PolyF-1** at the film thickness used. However, there are measurable fluorescence responses above the noise limit (3σ) of the spectrophotometer that better quantify the useful detection limit of the sensor. When this response is placed in a time domain, a correlation can be made between the time and H_2O_2 detection limits (Fig. 8). This plot correlates the proportional response

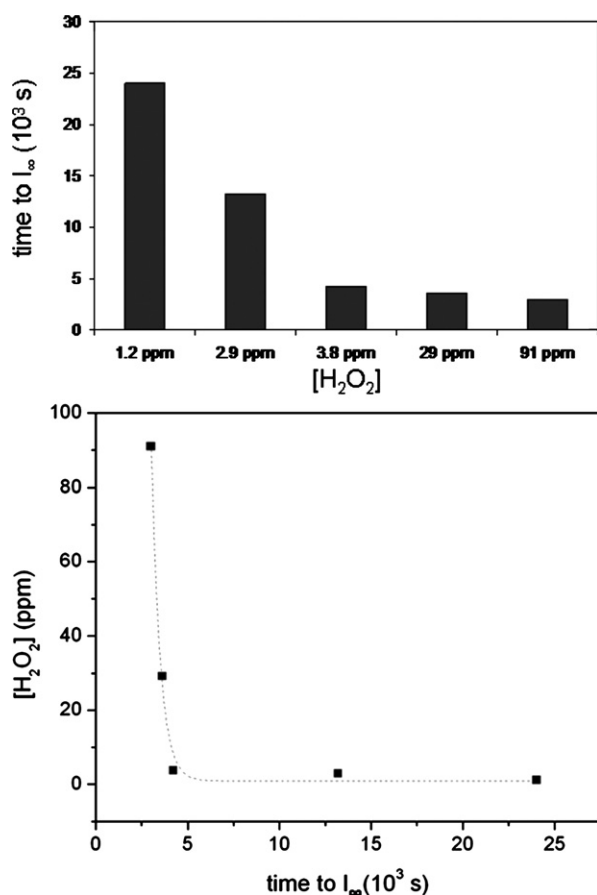


Fig. 7 Correlation between the concentration of H₂O₂ and the time to reach within 3σ of I_∞. I_∞ was calculated from the exponential growth fits of the time-dependent fluorescence traces at various concentrations of H₂O₂ observed in Fig. 3. The plot was fit to an exponential decay (eqn 2). A detection limit of 0.7 ppm H₂O₂ is calculated from the threshold reached by eqn 2. This detection limit is based on a maximum fluorescence response of **PolyF-1** to H₂O₂.

observed for the fluorescence intensity at 3σ above the noise of the spectrophotometer with the concentration of H₂O₂. The response is no longer an inverse response and therefore can provide more useful information on the detection capabilities of **PolyF-1**. The noise was calculated to be 0.08 from the fluorescence measurements taken of the **PolyF-1** film on exposure to UV light and ambient conditions (Fig. S1, ESI†). The data was fitted to a power function ($R^2 = 0.999$, eqn 3) as opposed to an exponential decay ($R^2 = 0.966$, eqn 2) to prevent a threshold limit from constraining the analysis. Using this equation, the time required to reach a desired detection limit can be calculated (Table 3). This plot is not limited by a maximum fluorescence intensity, revealing the low levels of detection that can be achieved with **PolyF-1**. For example, 9 ppb H₂O₂ can be detected after 3 h of exposure according to this analysis. A detection limit of 3 ppb is estimated to be possible after 8 h of exposure, which is two orders of magnitude below the permissible exposure limit (1 ppm) over an 8 h period established by OSHA.²² It is important to note, that these sensor films are effectively acting as integrating sensors for low levels of H₂O₂. This application may be useful in estimating average exposures over, for example, an

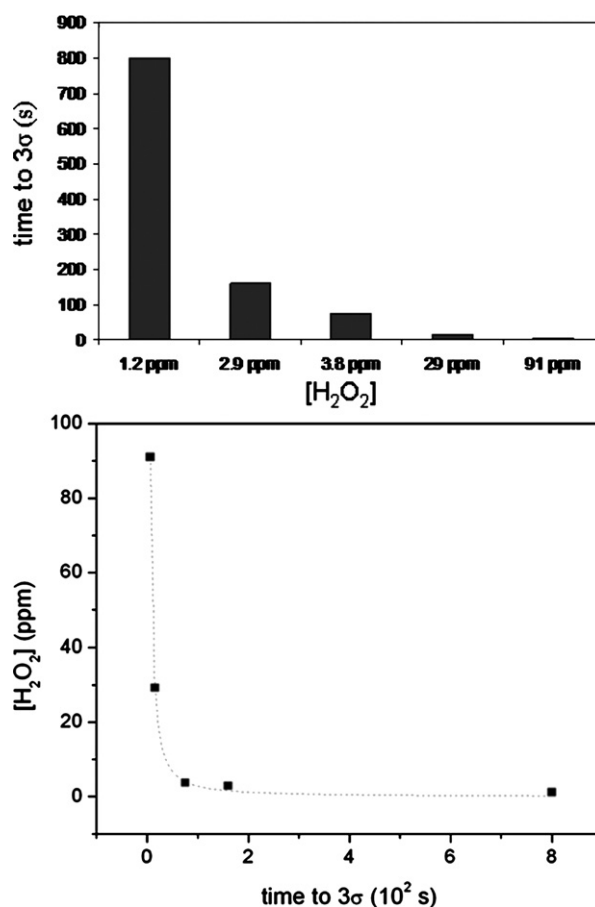


Fig. 8 Correlation between the concentration of H₂O₂ and the time to reach 3σ of the fluorescence response noise. The noise was calculated from the fluorescence response of **PolyF-1** to UV light over a 5 h period. The data was fit to a power function (eqn 3) providing the ability to calculate the time required to detect a desired concentration of H₂O₂ using a 10 μg cm⁻² film of **PolyF-1**.

Table 3 Time-dependent detection limits of H₂O₂ vapor by **PolyF-1** at various exposure times

Time/min	H ₂ O ₂ detection limit/ppb
10	300
60	30
180	9

8 h working shift or for monitoring the contents of shipping cargo containers for H₂O₂.

$$y = y_0 + A_1 e^{(x/t)} \quad (1)$$

$$y = y_0 + A e^{(-x/t)} \quad (2)$$

$$y = x^A \quad (3)$$

The high vapor pressure of H₂O₂ and the specificity that boronic esters show toward H₂O₂ oxidation¹⁹ make **PolyF-1** a highly sensitive and selective sensor for H₂O₂. The films show

little response to ambient conditions as well as UV light above the noise limit of the spectrophotometer over a 5 h period, indicating that radical oxygen species (ROS) and other oxidants found in the atmosphere as well as those that may be generated under a UV lamp ($\lambda = 302$ nm) are not interferences. The vapor pressures of most organic peroxides are much lower than for H_2O_2 , and thus are not significant interferences during vapor-phase detection. Many of these interferences, including various ROS and anionic species, have previously been tested in solution-phase studies and show little to no response.¹⁹ Besides its use as a vapor sensor, **PolyF-1** can also be used to screen suspicious liquids. This may be applicable to high throughput screening areas where concealed liquids would not produce a measurable vapor concentration of H_2O_2 . To test this application, solutions of H_2O_2 in water at various concentrations were spotted onto the same $10 \mu\text{g cm}^{-2}$ films of **PolyF-1** used during the vapor-phase

detection studies. Several common organic peroxides, including di-*t*-butylperoxide and benzoyl peroxide, were also spotted to confirm that the oxidative depolymerization of **PolyF-1** is insensitive to these interferences in spot tests (Fig. 9). **PolyF-1** easily detects 30 ppm of H_2O_2 during solution spot tests after 30 s. After 5 min, this signal increased further. Benzoyl peroxide (100 ppm) and di-*t*-butylperoxide (98%) show no detectable response after 5 min when spotted onto the **PolyF-1** film.

Conclusions

A new method of polymerization was developed using the double transesterification of arylboronates to synthesize **PolyF-1**. The chemical principle used to favor the polymer structure relies on the formation of six-membered boronic ester rings throughout the backbone from a monomer containing a five-membered boronic ester ring. This method of polymerization proved facile for the polymerization of fluoran and may be generalized to the polymerization of complex systems that are not compatible with boronic acid monomers. **PolyF-1** was designed and synthesized as a self-integrating sensor for the selective detection of vapor phase H_2O_2 by a fluorescence turn-on mechanism. H_2O_2 is an important by-product produced through thermal and UV degradation of the peroxide-based primary high explosives TATP and HMTD and its levels are also an occupational health and safety concern for its increasing use as a disinfectant and bleaching agent. Detection limits on the order of 3 ppb over an 8 h period can be achieved using thin films of **PolyF-1** on a porous sampling substrate. The detection process is insensitive to common interferences including organic peroxides and many ROS species. This technology can also be used to screen for H_2O_2 in suspicious liquids. A spot test of 30 ppm H_2O_2 shows visual detection within 30 s, with an increasing fluorescence response over time. The synthetic ease, stability, and processability of **PolyF-1** make it an ideal candidate for H_2O_2 detection applications that require a robust, low cost, sensitive, and selective sensor with rapid qualitative and semi-quantitative signal analysis.

Acknowledgements

This work was supported by the Air Force Office of Scientific Research (AFOSR-MURI #F49620-02-1-0288), RedXDefense (DHS subcontract 2006-0740R2), and the National Science Foundation (NSF-GRFP).

References

- (a) S. Singh, *J. Hazard. Mater.*, 2007, **144**, 15–28; (b) D. S. Moore, *Rev. Sci. Instrum.*, 2004, **75**, 2499–2512; (c) J. I. Steinfeld and J. Wormhoudt, *Annu. Rev. Phys. Chem.*, 1998, **49**, 203–232.
- (a) S. J. Toal and W. C. Trogler, *J. Mater. Chem.*, 2006, **16**, 2871–2883; (b) D. T. McQuade, A. E. Pullen and T. M. Swager, *Chem. Rev.*, 2000, **100**, 2537–2574; (c) J. C. Sanchez and W. C. Trogler, *J. Mater. Chem.*, 2008, **18**, 3143–3156; (d) J. C. Sanchez, S. A. Urbas, S. J. Toal, A. G. DiPasquale, A. L. Rheingold and W. C. Trogler, *Macromolecules*, 2008, **41**, 1237–1245; (e) J. C. Sanchez, A. G. DiPasquale, A. L. Rheingold and W. C. Trogler, *Chem. Mater.*, 2007, **19**, 6459–6470; (f) J. C. Sanchez, S. J. Toal, Z. Wang, R. E. Dugan and W. C. Trogler, *J. Forensic Sci.*, 2007, **52**, 1308–1313; (g) S. J. Toal, J. C. Sanchez, R. E. Dugan and W. C. Trogler, *J. Forensic Sci.*, 2007, **52**, 79–83.

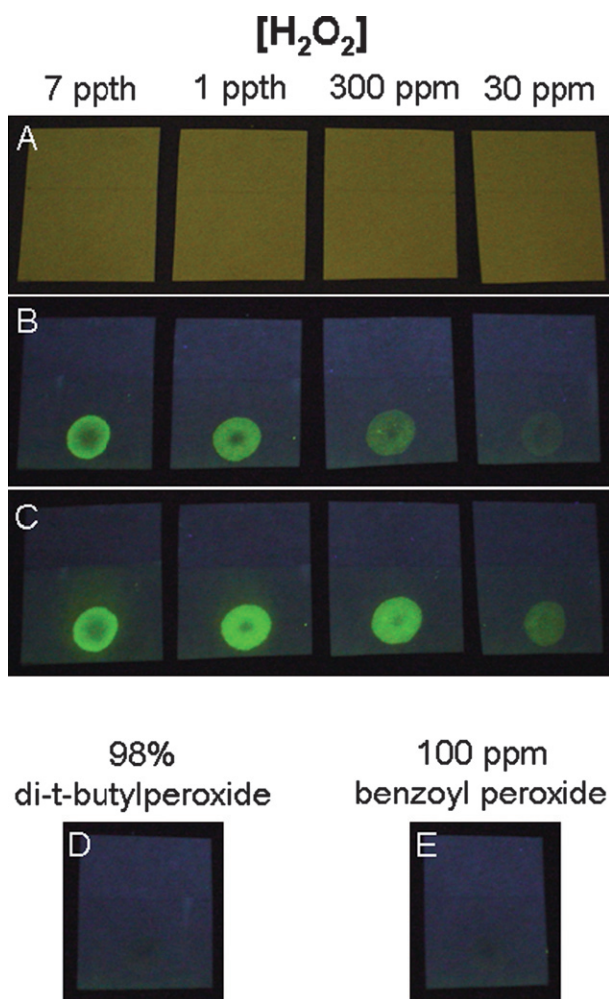


Fig. 9 Images of the fluorescence response of a $10 \mu\text{g cm}^{-2}$ film of **PolyF-1** to various solution concentrations of H_2O_2 and possible organic peroxide interferences. A) Film appearance under incandescent light. B) Detection of H_2O_2 under UV light (302 nm) after 30 s. C) Detection of H_2O_2 under UV light (302 nm) after 5 min. Detection increases over time. D) No fluorescence response observed for 98% di-*t*-butylperoxide after 5 min. E) No fluorescence response observed for 100 ppm benzoyl peroxide after 5 min.

- 3 (a) G. J. McKay, *Kayaku Gakkaishi*, 2002, **63**, 323–329; (b) G. M. White, *J. Forensic Sci.*, 1992, **37**, 652–656; (c) H. K. Evans, F. A. J. Tulleners, B. L. Sanchez and C. A. Rasmussen, *J. Forensic Sci.*, 1986, **31**, 1119–1125; (d) L. R. Ember, *Chem. Eng. News*, 2005, **83**, 11.
- 4 (a) B. T. Federoff, in *Encyclopedia of Explosives and Related Items*, ed. B. T. Federoff, H. A. Aaronson, E. F. Reese, O. E. Sheffield and G. D. Clift, Picatinny Arsenal, Dover, NJ, 1960, vol. 1, pp. A42–A45; (b) J. Yinon, *Forensic and Environmental Detection of Explosives*, John Wiley, Chichester, NY, 1999, pp. 10–11; (c) R. Meyer, J. Köhler and A. Homburg, *Explosives*, John Wiley-VCH, Weinheim, 5th edn, 2002, p. 346.
- 5 (a) J. C. Oxley, J. L. Smith and H. Chen, *Propellants, Explos., Pyrotech.*, 2002, **27**, 209–216; (b) J. C. Oxley, J. L. Smith, K. Shinde and J. Moran, *Propellants, Explos., Pyrotech.*, 2005, **30**, 127–130; (c) S. Zitrin, S. Kraus and B. Glatstein, *Proc. Int. Symp. Anal. Detect. Explos.*, FBI Academy, Quantico, VA, US, 1983, Federal Bureau of Investigation, Washington, DC, 1983, pp. 137–141.
- 6 For a recent review on the detection of peroxide-based explosives see: R. Schulte-Ladbeck, M. Vogel and U. Karst, *Anal. Bioanal. Chem.*, 2006, **386**, 559–565.
- 7 (a) J. G. Hong, J. Maguhn, D. Freitag and A. Ketrup, *Fresenius' J. Anal. Chem.*, 1998, **361**, 124–128; (b) R. Schulte-Ladbeck, P. Kolla and U. Karst, *Analyst*, 2002, **127**, 1152–1154.
- 8 H. Itzhaky and E. Keinan, *US Pat.*, US 6 767 717 B1, 2004.
- 9 (a) R. Schulte-Ladbeck, P. Kolla and U. Karst, *Anal. Chem.*, 2003, **75**, 731–735; (b) R. Schulte-Ladbeck, A. Edelmann, G. Quintas, B. Lendl and U. Karst, *Anal. Chem.*, 2006, **78**, 8150–8155; (c) P. van Zoonen, I. de Herder, C. Gooijer, N. H. Velthorst, R. W. Frei, E. Kuntzberg and G. Gubitzi, *Anal. Lett.*, 1986, **19**, 1949–1961; (d) J. Li and P. K. Dasgupta, *Anal. Chim. Acta*, 2001, **442**, 63–70; (e) R. Schulte-Ladbeck and U. Karst, *Anal. Chim. Acta*, 2003, **482**, 183–188; (f) J. Hong, J. Maguhn, D. Freitag and A. Ketrup, *Fresenius' J. Anal. Chem.*, 1998, **361**, 124–128; (g) Y. Yamamoto and B. N. Ames, *Free Radical Biol. Med.*, 1987, **3**, 359–361; (h) D. Lu, A. Cagan, R. A. A. Munoz, T. Tangkuaram and J. Wang, *Analyst*, 2006, **131**, 1279–1281; (i) E. Csoregi, L. Gorton, G. Marko-Varga, A. J. Tudos and W. T. Kok, *Anal. Chem.*, 1994, **66**, 3604–3610; (j) B. Sljukic, C. E. Banks and R. G. Compton, *Nano Lett.*, 2006, **6**, 1556–1558; (k) S. S. Kumar, J. Joseph and K. L. Phani, *Chem. Mater.*, 2007, **19**, 4722–4730; (l) D. F. Laine, C. W. Roske and I. F. Cheng, *Anal. Chim. Acta*, 2008, **608**, 56–60.
- 10 P. T. Jacobs and S. M. Lin, in *Irradiation of Polymers: Fundamentals and Technological Applications*, ed. R. L. Clough and S. W. Shalaby, ACS Symposium Series 620, American Chemical Society, Washington, DC, 1996, pp. 216–239.
- 11 (a) Occupational Safety and Health Administration Website, Chemical Sampling Information: Hydrogen Peroxide, http://www.osha.gov/dts/chemicalsampling/data/CH_246600.html (accessed May 2007); (b) K. F. Dickson and E. M. Caravati, *J. Toxicol., Clin. Toxicol.*, 1994, **32**, 705–714; (c) W. G. Proud and J. E. Field, *AIP Conf. Proc.*, 1999, **505**, 937–940; (d) O. Maass and W. H. Hatcher, *J. Am. Chem. Soc.*, 1920, **42**, 2548–2569.
- 12 (a) F. I. Bohrer, C. N. Colesniuc, J. Park, I. K. Schuller, A. C. Kummel and W. C. Trogler, *J. Mater. Chem.*, 2008, in press; (b) F. I. Bohrer, C. N. Colesniuc, J. Park, I. K. Schuller, A. C. Kummel and W. C. Trogler, *J. Am. Chem. Soc.*, 2008, **130**, 3712–3713.
- 13 Dräger Inc. Safety Website, DrägerSensor® H2O2 LC Chemical Sensor Data Sheet, http://www.draeger.com/ST/internet/pdf/Master/En/gt/9023492_h2o2lc_d_e.pdf (accessed July 2007).
- 14 (a) AFT International, Inc. Website, Dräger Safety Short Term Detector Tubes: Hydrogen Peroxide, <http://www.afcintl.com/pdf/draeger/8101041.pdf> (accessed July 2007); (b) M. A. Centanni, 'Visual detector for vaporized hydrogen peroxide', *US Pat.*, 7 186 373, 2003.
- 15 I. F. McVey, 'Non-dispersive mid-infrared sensor for vaporized hydrogen peroxide', *US Pat.*, 7 157 045, 2002.
- 16 (a) F. He, Y. Tang, M. Yu, S. Wang, Y. Li and D. Zhu, *Adv. Funct. Mater.*, 2006, **16**, 91–94; (b) F. He, F. Feng, S. Wang, Y. Li and D. Zhu, *J. Mater. Chem.*, 2007, **17**, 3702–3707.
- 17 H. Maeda, Y. Fukuyasu, S. Yoshida, M. Fukuda, K. Saeki, H. Matsuno, Y. Yamaguchi, K. Yoshida, K. Hirata and K. Miyamoto, *Angew. Chem., Int. Ed.*, 2004, **43**, 2389–2391.
- 18 (a) M. Onoda, T. Uchiyama, K. Mawatari, K. Kaneko and K. Nakagomi, *Anal. Sci.*, 2006, **22**, 815–817; (b) M. Onoda, H. Tokuyama, S. Uchiyama, K. Mawatari, T. Santa, K. Kaneko, K. Imai and K. Nakagomi, *Chem. Commun.*, 2005, 1848–1850.
- 19 (a) M. C. Y. Chang, A. Pralle, E. Y. Isacoff and C. J. Chang, *J. Am. Chem. Soc.*, 2004, **126**, 15392–15393; (b) E. W. Miller, A. E. Albers, A. Pralle, E. Y. Isacoff and C. J. Chang, *J. Am. Chem. Soc.*, 2005, **127**, 16652–16659; (c) E. W. Miller and C. J. Chang, *Curr. Opin. Chem. Biol.*, 2007, **11**, 620–625.
- 20 (a) Y. Li, J. Ding, M. Day, Y. Tao, J. Lu and M. D'iorio, *Chem. Mater.*, 2003, **15**, 4936–4943; (b) S. Maruyama and Y. Kawanishi, *J. Mater. Chem.*, 2002, **12**, 2245–2249; (c) Y. Chujo, I. Tomita and T. Saegusa, *Polym. J. (Tokyo, Jpn)*, 1991, **23**, 743–746.
- 21 (a) W. Niu, C. O'Sullivan, B. M. Rambo, M. D. Smith and J. J. Lavigne, *Chem. Commun.*, 2005, **34**, 4342–4344; (b) K. Koumoto, T. Yamashita, T. Kimura, R. Luboradzki and S. Shinkai, *Nanotechnology*, 2001, **12**, 25–31; (c) I. Nakazawa, S. Suda, M. Masuda, M. Asai and T. Shimizu, *Chem. Commun.*, 2000, 881–882; (d) E. I. Musina, I. A. Litvinov, A. S. Balueva and G. N. Nikonov, *Russ. J. Gen. Chem.*, 1999, **69**, 413–420.
- 22 (a) E. Barnea, T. Andrea, M. Kapon and M. S. Eisen, *J. Am. Chem. Soc.*, 2004, **126**, 5066–5067; (b) V. Barba, H. Hoepfl, N. Farfan, R. Santillan, H. I. Beltran and L. S. Zamudio Rivera, *Chem. Commun.*, 2004, 2834–2835; (c) N. Christinat, R. Scopelliti and K. Severin, *Chem. Commun.*, 2004, 1158–1159.
- 23 C. D. Roy and H. C. Brown, *J. Organomet. Chem.*, 2007, **692**, 784–790.
- 24 (a) G. Scatchard, G. M. Kavanagh and L. B. Ticknor, *J. Am. Chem. Soc.*, 1952, **74**, 3715–3720; (b) S. L. Manatt and M. R. R. Manatt, *Chem.–Eur. J.*, 2004, **10**, 6540–6557.
- 25 T. Ishiyama, K. Ishida and N. Miyaura, *Tetrahedron*, 2001, **57**, 9813–9816.